The AAPS Journal (2022) 24: 47
https://doi.org/10.1208/s12248-022-00698-x

RESEARCH ARTICLE

Targeted Delivery of Endosomal Escape Peptides to Enhance Immunotoxin Potency and Anti-cancer Efficacy

Joseph Ryan Polli[1] · Ping Chen[1] · Brandon M. Bordeau[1] · Joseph P. Balthasar[1]

Received: 6 January 2022 / Accepted: 5 March 2022 / Published online: 25 March 2022

Abstract

This work describes use of anti-carcinoembryonic antigen antibodies (10H6, T84.66) for targeted delivery of an endosomal escape peptide (H6CM18) and gelonin, a type I ribosome inactivating protein. The viability of colorectal cancer cells (LS174T, LoVo) was assessed following treatment with gelonin or gelonin immunotoxins, with or without co-treatment with T84.66-H6CM18. Fluorescent microscopy was used to visualize the escape of immunoconjugates from endosomes of treated cells, and efficacy and toxicity were assessed *in vivo* in xenograft tumor-bearing mice following single- and multiple-dose regimens. Application of 25 pM T84.66-H6CM18 combined with T84.66-gelonin increased gelonin potency by ~ 1,000-fold and by ~ 6,000-fold in LS174T and LoVo cells. Intravenous 10H6-gelonin at 1.0 mg/kg was well tolerated by LS174T tumor-bearing mice, while 10 and 25 mg/kg doses led to signs of toxicity. Single-dose administration of PBS, gelonin conjugated to T84.66 or 10H6, T84.66-H6CM18, or gelonin immunotoxins co-administered with T84.66-H6CM18 were evaluated. The combinations of T84.66-gelonin + 1.0 mg/kg T84.66-H6CM18 and 10H6-gelonin + 0.1 mg/kg T84.66-H6CM18 led to significant delays in LS174T growth. Use of a multiple-dose regimen allowed further anti-tumor effects, significantly extending median survival time by 33% and by 69%, for mice receiving 1 mg/kg 10H6-gelonin + 0.1 mg/kg T84.66-H6CM18 ($p = 0.0072$) and 1 mg/kg 10H6-gelonin + 1 mg/kg T84.66-H6CM18 ($p = 0.0017$). Combined administration of gelonin immunoconjugates with antibody-targeted endosomal escape peptides increased the delivery of gelonin to the cytoplasm of targeted cells, increased gelonin cell killing *in vitro* by 1,000–6,000 fold, and significantly increased *in vivo* efficacy.

KEY WORDS antibody · endosomal escape peptide · gelonin · immunotoxins · pH-sensitive

INTRODUCTION

Immunotoxins (ITs) contain a protein toxin chemically conjugated or genetically fused to a highly specific targeting domain, such as an antibody or antibody fragment (1–3). The protein toxins most commonly employed for ITs belong to a class of molecules known as ribosome inactivating proteins (RIPs) (4–6). Early publications demonstrated that cytoplasmic delivery of a single RIP molecule, such as abrin, ricin, and modeccin (7), induces cellular apoptosis. RIP molecules are categorized as Type-I or Type-II agents, based on the presence or absence of domains mediating cell entry and endosomal escape, which are key determinants of RIP potency. For example, gelonin, a Type-I RIP, lacks domains for cell entry and endosomal escape and, consequently, gelonin is associated with poor potency when applied in cell culture and with a high (> 40 mg/kg) median lethal dose (LD_{50}) when administered to mice. By contrast, Type-II RIPs such as *pseudomonas* exotoxin A and ricin, which include cell entry and endosomal escape domains, exhibit LD_{50} values of ~ 1 μg/kg in mice (8, 9).

Due to low potential for induction of systemic toxicity and high potential for catalytic ability following delivery to the cytoplasm, there has been substantial interest in the development of gelonin immunotoxins for treatment of cancer (10). Although several gelonin immunotoxins have been reported in the literature, only a single modality has entered clinical studies, HUM-195/rGEL (NCT00038051). Unfortunately, this construct failed to progress due to modest clinical efficacy (11). In a comprehensive study of gelonin immunotoxins, the Wittrup laboratory reported that internalization of ~ 5 million molecules of gelonin is required to

✉ Joseph P. Balthasar
jb@buffalo.edu

[1] Department of Pharmaceutical Sciences, School of Pharmacy and Pharmaceutical Sciences, University at Buffalo, Buffalo, New York 14214, USA

induce apoptosis, regardless of the structure of the gelonin immunoconjugate (12). Given that cell death can be mediated by a single gelonin molecule delivered to the cytoplasm, inefficient endosomal escape was identified as a key limiting factor for gelonin immunotoxins. Consistent with endosomal escape limiting gelonin efficacy, mathematical modeling by Yazdi et al. predicted that for every 10 million endocytosed gelonin molecules, only one gelonin molecule enters the cytosol (13).

Membrane penetrating agents known as cell-penetrating peptides, or protein transduction domains (PTD), have been identified for their ability to translocate macromolecule payloads across biological membranes (14, 15). A subclass of cell-penetrating peptides known as endosomal escape peptides (EEPs) exhibit pH-dependent activity. GALA, INF7, and H5WYG are well-described EEPs that include amino acid residues with pKa values similar to the pH of acidified endosomes (~ 5.0–6.0), allowing transition from a neutral charge in extracellular fluid (at physiological pH) to a positive charge in endosomes, and promoting membrane interaction (16–18). Considering the small size and ability to disrupt membranes in a pH-dependent manner, EEPs may be suitable for potentiating the efficacy of immunotoxins.

A particular subclass of mAbs with pH-dependent antigen binding, termed "catch-and-release" (CAR) mAbs, exhibit high affinity target binding at physiologic pH (pH 7.4), and negligible target binding at mildly acidic pH (pH 5.5—6.0). CAR mAbs have been employed for several applications due to their ability to reduce target-mediated mAb elimination (i.e., enhancing exposure) (19–22). Recently, we have generated an IgG1κ murine CAR mAb (10H6) against a tumor-associated antigen, carcinoembryonic antigen (CEA), by standard mouse hybridoma technology. When compared to anti-CEA mAb with "standard" (i.e., pH-independent) binding, 10H6 demonstrated decreased target-mediated elimination and increased tumor exposure in the $MC38^{CEA+}$ mouse model of murine colorectal cancer (22). Considering the unique binding properties of 10H6, we hypothesized that immunoconjugates developed with CAR mAbs may be employed to enhance the endosomal escape and cytoplasmic delivery of macromolecular toxins. The proposed strategy employs a combination of two conjugates: 1) CAR-EEP and 2) CAR-toxin (Fig. 1). Co-administration of CAR-toxin and CAR-EEP was expected to allow membrane accumulation, and subsequent internalization of both constructs into endosomes. Acidification of the endosomal matrix results in release of CAR-EEP from the membrane-associated target, allowing EEPs to interact with endosomal membranes, facilitating pore-formation and membrane lysis. Simultaneously, CAR-toxin that has dissociated from the

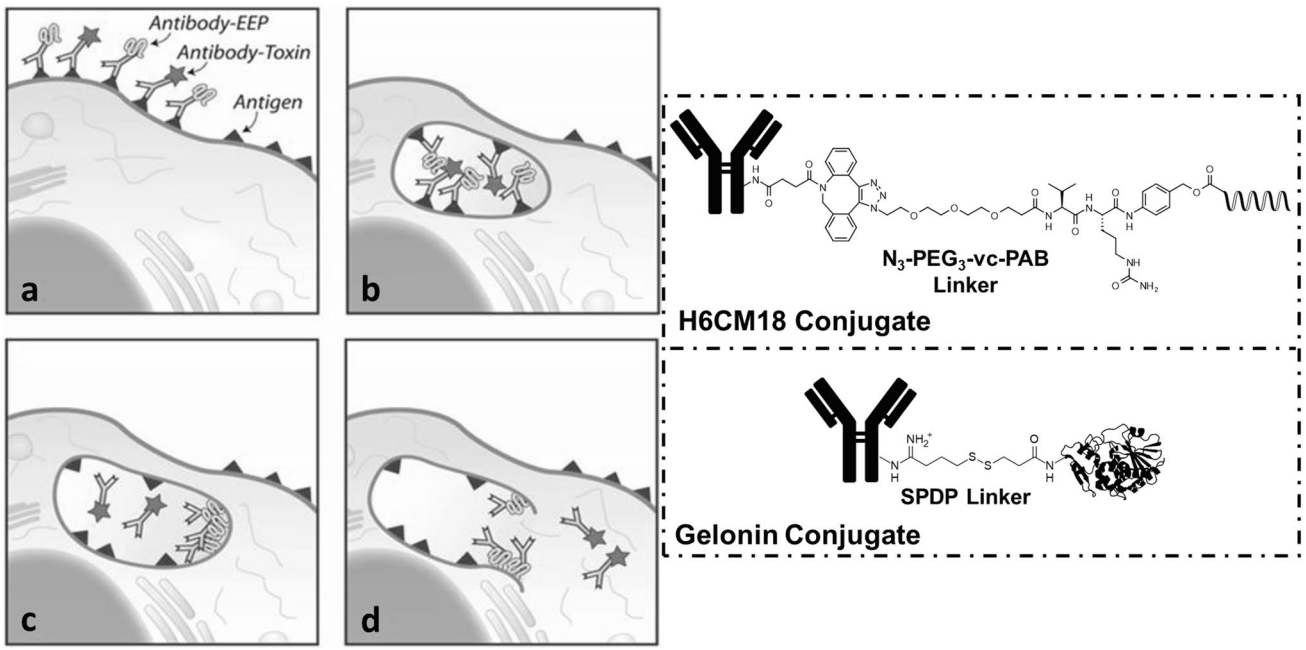

Fig. 1 Use of catch-and-release (CAR) antibody conjugates to promote the endosomal escape of cell-targeted toxins.(Left) Mechanistic diagram of the CAR conjugate strategy. **a** Anti-CEA immunoconjugates bind to CEA-expressing colorectal cancer cells, **b** CEA-bound immunoconjugates are internalized via receptor mediated endocytosis into early endosomes. **c** Maturation and acidification of endosomes allows CAR mAbs to release from target and promote interaction of EEP conjugates to endosomal membranes. **d** Following pore formation and subsequent lysis, CAR-gelonin may diffuse out of the endosome directly into the cytosol where gelonin can deactivate ribosomes. (Right) Schematic of the chemical linkers employed to conjugate either macromolecular toxin, gelonin, or EEP to antibody. H6CM18 is linked to mAb by a N_3-PEG_3-vc-PABC linker with use of Cu^{2+}-free click chemistry. Gelonin is linked to mAb via an SPDP linker that requires reduction of the disulfide bond to release the toxin

membrane-associated target will be freely available to diffuse through pores formed by CAR-EEPs into the cytosol, where the toxin (e.g., gelonin) can mediate cell killing (e.g., via deactivation of ribosomes). As an alternative approach, we propose that efficient endosomal release within targeted cells may be facilitated through the use of cleavable linker chemistry, as developed within the antibody–drug conjugate field. Combined, targeted delivery and endosomal release of macromolecular toxins and EEP, either by use of CAR-mAb or by use of cleavable linkers, is expected to provide the combined attributes of high therapeutic selectivity and high potency. The present work tests this hypothesis through the development, characterization, *in vitro* and *in vivo* evaluation of mAb conjugates with EEP and gelonin.

MATERIALS AND METHODS

Colorectal Cancer Cell Lines

Two human colorectal cancer cell lines with high expression of membrane bound CEA, LS174T and LoVo, were employed in these studies. Both cell lines were purchased from the American Type Culture Collection (ATCC, Manassas, VA). LS174T (CL-188) is a human colorectal adenocarcinoma that expresses 2×10^6 molecules of CEA per cell (23), and LoVo (CCL-299) is a human colorectal adenocarcinoma that expresses 3×10^6 molecules of CEA per cell (24).

Natural Gelonin and Expression of Recombinant Gelonin

Natural gelonin (nGel) was purchased from Enzo (Farmingdale, NY). Recombinant gelonin (rGel) amino acid sequence was obtained from UniProt (ID# P33186). The corresponding DNA was optimized and synthesized by GenScript®. Following ligation into pET21b, rGel was produced through culture of transfected *E. coli* (strain Shuffle, New England Biolabs, Ipswich, MA, C3029J), and then separated from contaminating proteins using a Bio-Scale Mini CHT Cartridge (BioRad, Hercules, CA, 7324324). Purity was assessed by sodium dodecyl sulfate–polyacrylamide gel electrophoresis (SDS-PAGE) and Western blot analysis.

Antibody Conjugation to Gelonin and Endosomal Escape Peptides

10H6 and T84.66 were purified as described previously (22). Gelonin (i.e. nGel or rGel) was cross-linked to anti-CEA antibodies using a disulfide linker SPDP based on previous methods (25). After the conjugation, gelonin conjugates were buffer exchanged into 20 mM Na_2HPO_4, pH 7.0 followed by protein G purification. Gelonin conjugates were assessed for purity and drug-to-antibody ratio by SDS-PAGE (Fig. S2) and ELISA (26).

The H6CM18 peptide (described below) was custom-synthesized by ThermoFisher with a N_3-PEG_3-vc-PABC linker attached to the N-terminus. Addition of a terminal azide group allows conjugation to antibody by Cu^{2+}-free Click-Chemistry (27). T84.66 was functionalized with dibenzocyclooctyne-*N*-hydroxysuccinimidyl ester (DBCO-NHS, Sigma-Aldrich, St. Louis, MO, 761524) by reacting at either 1:20 (high modification) or 1:5 (low modification) molar equivalents for 15 min at room temperature with constant mixing in PBS. The reaction was quenched by spiking in 1 M Tris–HCl, pH 9.0 to a final concentration of 75 mM for 7 min. After quenching, the reaction was desalted into PBS and reacted with peptide at either 1:10 or 1:4 molar ratio (Ab:peptide) overnight at 4 °C. For site-specific conjugation, 3 mg of T84.66 in Dulbecco's PBS was first reduced with 3.67 molar equivalents of 10 mM Tris(2-carboxyethyl)phosphine hydrochloride (TCEP) for 2 h at 37 °C in a polystyrene tube. Following TCEP reduction, free thiol groups were measured using 5,5-dithio-bis-(2-nitrobenzoic acid) (DTNB) (ThermoFisher, Grand Island, NY, 22582). Reduced antibody was reacted at room temperature for 1 h with 1:8 molar ratio DBCO-PEG_4-Maleimide (Click Chemistry Tools, Scottsdale, AZ, A108P-25), where maleimide will react with free thiol groups of the antibody. This reaction was quenched by buffer exchanging into DPBS and then reacted overnight at 4 °C with 4 molar equivalents of N_3-PEG_3-vc-PAB-H6CM18, in 20% v/v DMF to prevent linker precipitation during reaction. Lysine and cysteine modification reactions were desalted and dialyzed into PBS, where peptide conjugation was confirmed by ELISA using CEA coated plates to capture anti-CEA antibody and detected with an anti-6xHis-alkaline phosphatase conjugate, which recognizes the hexahistidine sequence on H6CM18.

Cell Viability Assessments

Log-phase CEA-expressing cell lines were seeded in 96-well microtiter plates at 2500 cells/well (LS174T) or 5000 cells/well (LoVo) in 175 µL of culture medium. Cells were allowed to adhere for 24 h before cell culture media was aspirated and replaced with 200 µL of fresh media containing a range of treatment and control concentrations. After a 72-h treatment period, cells were washed three times with 200 µL of fresh media. Following the final wash, 100 µL of complete media and 25 µL of 3-(4,5-dimethylthiazol-2-yl)-2,5-diphenyltetrazolium bromide (MTT) (Sigma, St. Louis, MO) solution (5 mg/mL in pH 7.4 1xPBS) were added and incubated for 4 h in order to allow cells to reduce MTT to formazan dye. After MTT reduction, 100 µL of 10% SDS prepared in 0.01 M HCl was added to each well and incubated overnight to solubilize the formazan crystals.

Formazan dye was measured at 590 nm and normalized by cell debris at 640 nm (Spectromax, Molecular Devices, Sunnyvale, CA). Half-maximal inhibitory concentration values (IC_{50}) were determined by fitting a cell growth inhibition model with variable slope using GraphPad Prism 7.04 (GraphPad Software, Inc).

Fluorescent Microscopy

LS174T cells were seeded in 35 mm Glass bottom dishes with 10 mm micro-well cover glass (CellVis, Mountain View, CA, D35-10–1-N) at the density of 3000 cells/coverslip for 24 h. Then culture medium was replaced with 100 nM Alexa Fluor 680 labeled 10H6-gelonin with or without 50 nM T84.66-H6CM18. After 24-h incubation, cells were washed with Live Cell Imaging Solution (LCIS, Invitogen, Grand Island, NY, A14291DJ) and incubated with pHrodo Green (Invitrogen, Grand Island, NY) at 40 µg/ml in LCIS at 37 °C for 30 min. Meanwhile, two drops/ml of NucBlue® Live ReadyProbes® Reagent (Invitrogen, Grand Island, NY, R37605) was added into LCIS. Afterwards, cells were washed twice with ice-cold LCIS. A Leica DMi 8 inverted fluorescence microscope equipped with a 63 × oil immersion objective was used for live cell imaging. Cells were imaged in bright-field, or fluorescence with DAPI, GFP and LED-QUAD excitation cubes for detection of nuclei, endosomes, and 10H6-gelonin, respectively. 3D images with z stacks were acquired and 3D deconvolution processing was conducted using the autoquant blind deconvolution software integrated into LAS X software. Colocalization between 10H6-gelonin and endo/lysosome was visualized using 2D intensity histogram and quantitatively assessed using the Pearson's correlation coefficient (PCC) (28, 29), using the plugin Coloc 2 in the Fiji software®. PCC close to 1 indicates fluorescence intensities of two channels are perfectly linearly related, near 0 represents the two fluorescence intensities are uncorrelated and -1 means perfect negative correlation.

Toxicity Assessment of 10H6-rGel

Male athymic nude mice, 4–6 weeks (Jackson Laboratory, Bar Harbor, ME), received subcutaneous injections of ~ 10^6 LS174T in the left flank. 10H6-rGel was administered at 1, 10, or 25 mg/kg intravenously via the retro-orbital sinus plexus when tumor sizes reached 200–300 mm^3. Mice were assigned to treatment groups by a single blind randomization (n = 3). Tumor volumes were calculated as: $0.5 \bullet l \bullet w^2$, where "l" represents the longest diameter of the tumor and "w" represents the diameter perpendicular to "l". Mice were euthanized if tumor diameter exceeded 20 mm, or in cases of tumor ulceration, weight loss > 15%, or in cases where mice exhibited signs of pain or distress.

In vivo Efficacy

Male athymic nude mice (The Jackson Laboratory, Bar Harbor, ME) received subcutaneous injections of ~ 10^6 LS174T. Single-dose efficacy was assessed with 1 mg/kg T84.66-rGel or 10H6-rGel administered alone or with either 0.1 or 1 mg/kg T84.66-H6CM18, intravenously, via the retro-orbital sinus plexus of mice bearing 200–300 mm^3 tumors. Mice were assigned to treatment groups by a single blind randomization (n = 5). In a multiple-dose efficacy study (n = 6/group), 10H6-rGel was administered to ~ 100 mm^3 tumor-bearing mice at 1 mg/kg with either 0.1 or 1 mg/kg T84.66-H6CM18, every four days, intravenously, via the retro-orbital sinus plexus. Tumor volumes were calculated as described above.

RESULTS

Enhancement of nGel Potency by H6CM18

His-CM_{18}-PTD4 is a chimeric peptide that consists of amino acid residues 1–7 of cecropin-A, 2–12 of melittin, 47–57 of TAT variant PTD4, and an N-terminal hexahistidine tag (30–32). This peptide has shown great utility in mediating delivery and endosomal escape of CRISPR/Cas9 components and up to 250 kDa fluorescent dextrans to cells (32). In order to evaluate this peptide for our delivery strategy, we truncated His-CM_{18}-PTD4 to His-CM_{18} (hereon referred to as H6CM18) and added a cathepsin B cleavable linker, vc-PABC (33), to facilitate conjugation to mAb and to enable release of native (i.e., unmodified) membrane lytic peptide following proteolytic cleavage in cellular endosomes. Conjugation was achieved by employing Cu^{2+}-free click chemistry, where the vc-H6CM18 linker contains a PEG_3 spacer with a terminal azide functional group. We have opted to use T84.66 for development of H6CM18 conjugates due to the high affinity for CEA and use of a protease cleavable linker. Modification of T84.66 lysine residues by NHS-DBCO resulted in superior peptide load when compared to conjugates prepared by site-specific cysteine modification. ELISA using an anti-hexahistidine tag antibody conjugated with alkaline phosphatase enzyme confirmed this modification (Fig. S3A).

Initial cytotoxicity evaluations with LS174T colorectal cancer cells were performed using 10H6-nGel combined with T84.66-H6CM18 (high modification). The combination improved the IC_{50} value of 10H6-nGel from 1040 to 34.9 nM (400:1 ratio of 10H6-nGel:T84.66-H6CM18) and 164 nM (10H6-nGel + fixed 50 nM T84.66-H6CM18) (Fig. 2a, Table I). T84.66-H6CM18 alone did not exhibit any cytotoxicity up to 100 nM (Fig. S3B). Competitive flow cytometry analyses showed no competition between

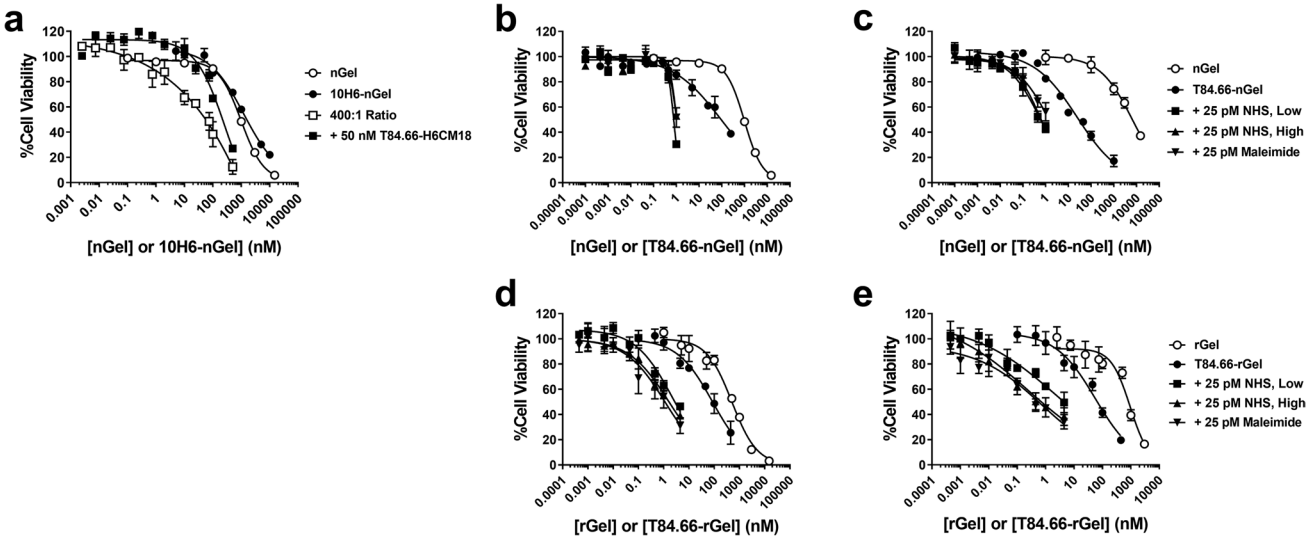

Fig. 2 Cell viability assays evaluating the combination strategy utilizing T84.66-H6CM18 as a potentiator. **a** Cell viability assay with LS174T cells evaluating 10H6 targeted nGel in presence of T84.66-H6CM18 (NHS, high modification) nGel and 10H6-nGel are presented in open circles and black circles. 10H6-nGel and T84.66-H6CM18 were incubated at either a constant 400:1 ratio (open squares), based on K_D difference, or a fixed 50 nM concentration of T84.66-H6CM18 (closed squares). T84.66-nGel (closed circles) was evaluated with low modification of NHS (closed squares), high modification NHS (closed upright triangles), and site-specific chemistry using maleimide modification (closed inverse triangles) in **b** LS174T and **c** LoVo colorectal cancer cell models. T84.66-rGel was evaluated with all three T84.66-H6CM18 conjugates in **d** LS174T and **e** LoVo colorectal cancer cell models. Free gelonin (open circles) are provided for comparison. Symbols represent mean cell viability and bars represent standard deviation of the mean

Table I LS174T Cell Cytotoxicity of mAb-Gelonin in Presence of T84.66-H6CM18. 10H6-Gel or T84.66-Gel were evaluated with low modification of NHS, high modification NHS, and site-specific chemistry using maleimide modification in LS174T colorectal cancer cell models. Table includes IC50, CV% and 95% confidence interval. Cell cytotoxicity data of free rGel, free nGel and T84.66-H6CM18 are provided for comparison

Treatment Condition	IC_{50} (nM)	CV%	CI (95%)
nGel	1040	4.93	[937 – 1150]
10H6-nGel*	1330	11.0	[1040 – 1650]
T84.66-H6CM18	N.D	N.D	N.D
400:1 (10H6-nGel:T84.66-H6CM18)*	34.9	17.1	[23.4 – 49.4]
10H6-nGel + 50 nM T84.66-H6CM18*	164	9.00	[128 – 214]
T84.66-nGel*	94.6	17.3	[68.2 – 138]
+ 25 pM T84.66-H6CM18 (NHS, Low)*	1.05	4.90	[0.955 – 1.19]
+ 25 pM T84.66-H6CM18 (NHS, High)*	0.769	4.67	[0.698 – 0.846]
+ 25 pM T84.66-H6CM18 (Maleimide)*	1.05	4.95	[0.958 – 1.19]
rGel	504	9.68	[411 – 615]
T84.66-rGel*	86.5	20.0	[58.7 – 133]
+ 25 pM T84.66-H6CM18 (NHS, Low)*	2.19	13.2	[1.69 – 2.93]
+ 25 pM T84.66-H6CM18 (NHS, High)*	1.63	12.2	[1.28 – 2.10]
+ 25 pM T84.66-H6CM18 (Maleimide)*	1.13	35.7	[0.581 –2.67]

** statistical significance of T84.66-H6CM18 combination compared to gelonin based on extra sum-of-squares F-test, $p < 0.05$*

T84.66 and 10H6 for binding to CEA + cells (Fig. S4), indicating the ~ 30-fold enhancement in gelonin potency with 10H6-nGel + T84.66-H6CM18 combination is most likely due to the moderate/low binding affinity of 10H6-nGel (i.e., $K_{D,10H6} = 10$ nM).

Due to expectations for direct competition between the T84.66 conjugates, T84.66-H6CM18 was applied at a fixed concentration of 25 pM in combination with T84.66-nGel. Based on T84.66 affinity for CEA, it is expected that the 25 pM concentration of T84.66-H6CM18 will achieve ~ 75% CEA occupancy. This combination lowered the IC_{50} of nGel from 1040 nM to 0.769 nM in LS174T cells (Fig. 2b, Table I). Although high modification of T84.66 enhanced potency of gelonin, this conjugate tended to precipitate;

therefore, a lower modification ratio was used to develop a more viable peptide conjugate for *in vivo* applications. In addition, a maleimide activated DBCO reagent was used to react with free thiol groups of reduced T84.66 to develop site-specific conjugates. T84.66-H6CM18 (NHS, low or maleimide) in combination with T84.66-nGel increased potency of gelonin to 1.05 nM (Fig. 2b). The combination was evaluated in a second colorectal cancer cell line, LoVo. nGel exhibited an IC_{50} value of 6.48 μM, which was lowered by conjugation to T84.66 to 24.6 nM. In combination with NHS-low, NHS-high, and maleimide T84.66-H6CM18, the IC_{50} value further decreased to less than 1 nM (Fig. 2c and Table II).

Enhancement of rGel Potency by H6CM18

For *in vivo* application, prior reports have demonstrated specific macrophage and liver sinusoidal endothelial cell receptors (e.g., mannose receptor) recognize carbohydrate moieties expressed on nGel, which can potentially lead to liver toxicities and vascular leak syndrome. To prevent non-specific uptake of gelonin immunotoxins *in vivo*, gelonin was expressed recombinantly in *E. coli*, where expressed proteins lack any glycosylation. rGel was successfully expressed and purified with moderate yield (~ 1.5 mg/L) (Fig. S1A) and high purity following CHT hydroxyapatite chromatography (> 95% by SDS-PAGE and Western blot) (Fig. S1B). T84.66 immunotoxins were synthesized successfully and purified using Protein G chromatography (Fig. S1C). rGel and T84.66-rGel were first evaluated in LS174T colorectal cancer cells and demonstrated IC_{50} values of 504 nM and 86.5 nM, respectively. T84.66-H6CM18 enhanced the potency of T84.66-rGel to 2.19, 1.63 or 1.13 nM (NHS low, NHS high, and maleimide, respectively) (Fig. 2d, Table I). In LoVo colorectal cancer cells, rGel exhibited an IC_{50} of 948 nM, similar to that of nGel, while T84.66-rGel also displayed a similar IC_{50} value of 56.9 ± 8.48 nM (Fig. 2e, Table II). In combination with low and high modification T84.66-H6CM18, the IC_{50} values decreased to 2.13 nM and 0.249 nM, while site-specific H6CM18 conjugates exhibited an IC_{50} of 0.750 nM (Fig. 2e, Table II). These results, shown in two colorectal cancer cell models, demonstrate that T84.66-H6CM18 potentiated gelonin cytotoxicity by > 6,000-fold.

Endosomal Escape Potentiation by H6MC18

To assess the impact of T84.66-H6CM18 on the distribution of gelonin from endosomes, LS174T cells were incubated with 10H6-gelonin-Alexafluor 680 alone or in combination with T84.66-H6CM18 for 24 h. The pH-sensitive fluorescent dye pHrodo-green was used to identify endosomes and lysosomes (34, 35), as pHrodo is non-fluorescent at neutral pH, but brightly fluorescent at acidic pH. Cells were imaged by fluorescence microscopy. Most of the 10H6-gelonin (red) colocalized with pHrodo-green, as displayed in yellow (Fig. 3a), with a small fraction of 10H6-gelonin found outside of endosomes (Figure S5A-S5D). However, following co-incubation with T84.66-H6CM18, a large quantity of 10H6-gelonin escaped endosomes (Fig. 3b, Figure S5E-H). To assess the correlation of pixel intensities of 10H6-gelonin and endo-/lysosomes, 2D intensity histograms were generated (Fig. 3c & d), and the colocalization between the two fluorescent signal was quantified by Pearson's correlation coefficient (PCC) analysis. The PCC value of 10H6-gelonin alone was 0.544 ± 0.137, while in combination with T84.66-H6CM18, the PCC was 0.110 ± 0.136. The significant decrease in PCC ($p = 0.0010$) demonstrates that T84.66-H6CM18 enhances the endosomal escape of 10H6-gelonin (Fig. 3e).

Table II LoVo Cell Cytotoxicity of T84.66-Gelonin in Presence of T84.66-H6CM18. T84.66-Gel were evaluated with low modification of NHS, high modification NHS, and site-specific chemistry using maleimide modification in LoVo colorectal cancer cell models. Table includes IC50, CV% and 95% confidence interval. Cell cytotoxicity data of free rGel and free nGel are provided for comparison

Treatment Condition	IC_{50} (nM)	CV%	CI (95%)
nGel	6480	12.6	[4900 – 8530]
T84.66-nGel*	24.6	15.5	[18.0 – 33.4]
+ 25 pM T84.66-H6CM18 (NHS, Low)*	0.594	9.57	[0.492 – 0.724]
+ 25 pM T84.66-H6CM18 (NHS, High)*	0.677	7.55	[0.584 – 0.793]
+ 25 pM T84.66-H6CM18 (Maleimide)*	1.49	17.8	[1.10 – 2.24]
rGel	948	9.39	[747 – 1140]
T84.66-rGel*	56.9	14.9	[40.2 – 76.7]
+ 25 pM T84.66-H6CM18 (NHS, Low)*	2.127	27.1	[1.02 – 3.44]
+ 25 pM T84.66-H6CM18 (NHS, High)*	0.249	76.4	[0.00854 – 0.713]
+ 25 pM T84.66-H6CM18 (Maleimide)*	0.750	32.2	[0.298 – 1.31]

**statistical significance of T84.66-H6CM18 combination compared to gelonin based on extra sum-of-squares F-test, $p < 0.05$*

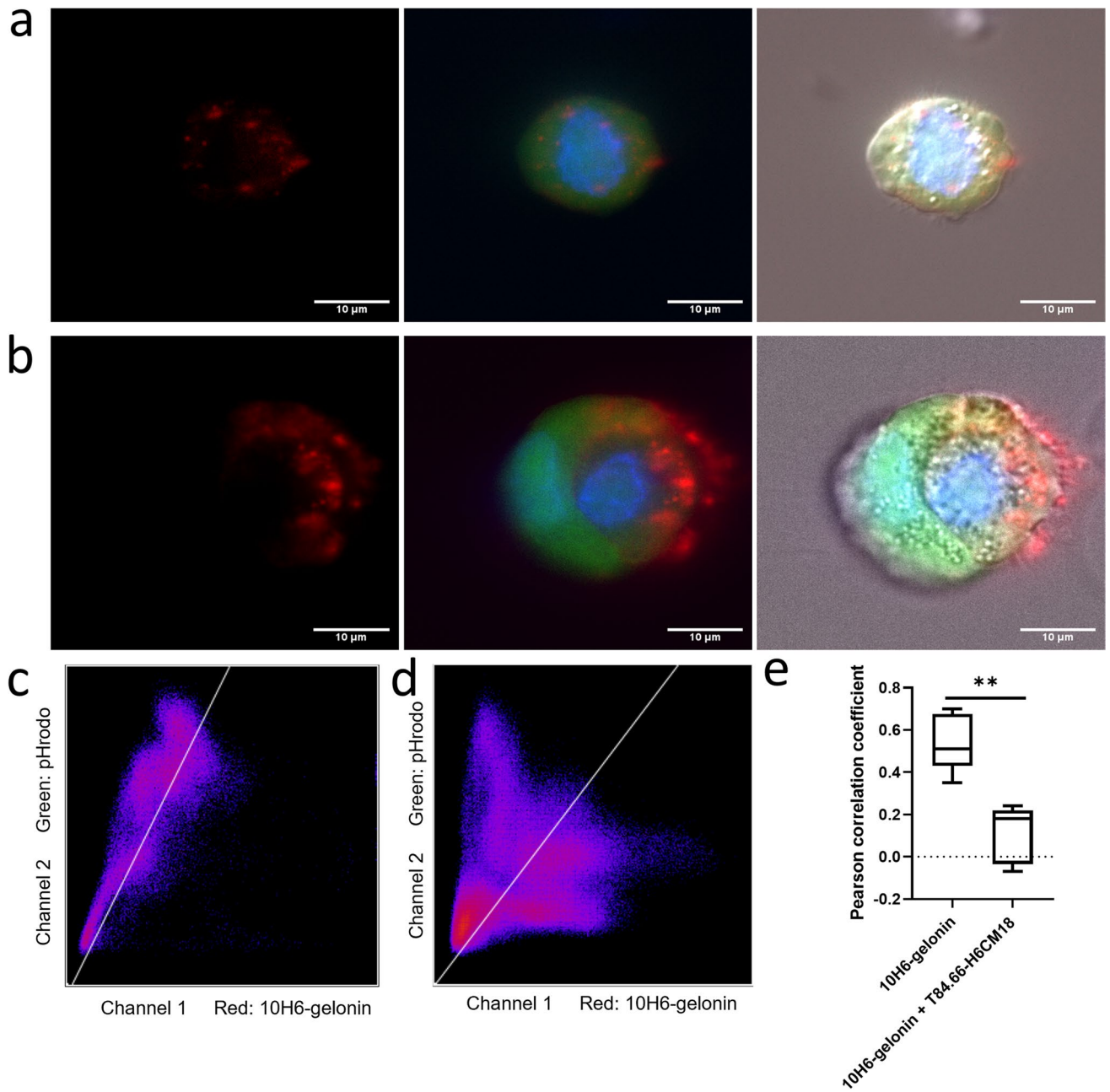

Fig. 3 Endosomal escape of CAR conjugate strategy by fluorescent microscope. Representative fluorescence images of LS174T cells incubated with **a** 10H6-gelonin alone or **b** 10H6-gelonin in combination of T84.66-H6CM18. 10H6-gelonin was labeled with Alexa fluor 680 (red), endosomes/lysosomes were stained with pHrodo-green (green), and nuclei was stained with NucBlue® Live ReadyProbes® Reagent (blue). Merged green and red particles were shown as yellow. Representative 2D intensity histogram of green fluorescence and red fluorescence in the condition of **c** 10H6-gelonin alone (PCC = 0.51) or **d** 10H6-gelonin in combination of T84.66-H6CM18 (PCC = 0.20). **e** Co-localization coefficient (PCC ± SD) between the red and green fluorescence intensity. (10H6-gelonin: N = 5 fields, 55 cells; 10H6-gelonin + T84.66-H6CM18: N = 5 fields, 92 cells). 2D intensity histogram and PCC analysis were generated by Coloc2 in Fiji

Dose Optimization-Toxicity Assessment

Prior to evaluating *in vivo* efficacy of rGel immunotoxins and T84.66-H6CM18, 10H6-rGel immunotoxins were evaluated, following a range of doses, in LS174T xenograft-mice. Doses of 1, 10, and 25 mg/kg were selected based on prior published work with gelonin immunotoxins (36, 37). Tumor burden in response to 10H6-rGel treatment was similar across all treatments. Interestingly, 25 mg/kg of either 10H6 or 10H6-rGel demonstrated a minor delay in tumor growth

as compared to the PBS control (Fig. 4a). For mice treated with 25 mg/kg doses of 10H6-rGel, significant adverse events were observed within 4 days after treatment, as mice lost > 15% body weight (Fig. 4b) or demonstrated signs of distress (e.g., cold skin and arching backs). Due to occurrence of adverse events, all mice were euthanized by day 6 (Fig. 4c). 10H6-rGel at 10 mg/kg caused an average decrease in body weight of ~ 6%, with one mouse losing > 15% body weight by day 3. Animals treated with 1 mg/kg 10H6-rGel exhibited no observable adverse events and no decreases in body weight (Fig. 4b). A Kaplan–Meier survival analysis demonstrated a slight trend toward increased survival in comparisons of 10H6 and 10H6-rGel at 25 mg/kg *vs.* PBS treatment, but survival differences were not statistically significant (Fig. 4c, $p = 0.419$). mAb-rGel at 1 mg/kg was selected for use in subsequent combination studies, as no adverse events were observed following administration of 10H6-rGel at this dose.

EEP/IT Single-dose Efficacy Evaluation

10H6-rGel and T84.66-rGel were evaluated for efficacy in mice bearing LS174T tumors, following doses of 1 mg/kg, administered alone or in combination with 0.1 or 1 mg/kg T84.66-H6CM18. Animals treated with T84.66-rGel and 10H6-rGel alone demonstrated similar tumor growth as found with administration of PBS, indicating a lack of benefit from treatment of 1 mg/kg immunotoxin alone (Fig. 5a). Mice treated with T84.66-rGel in combination with T84.66-H6CM18 at 0.1 mg/kg also demonstrated a similar tumor

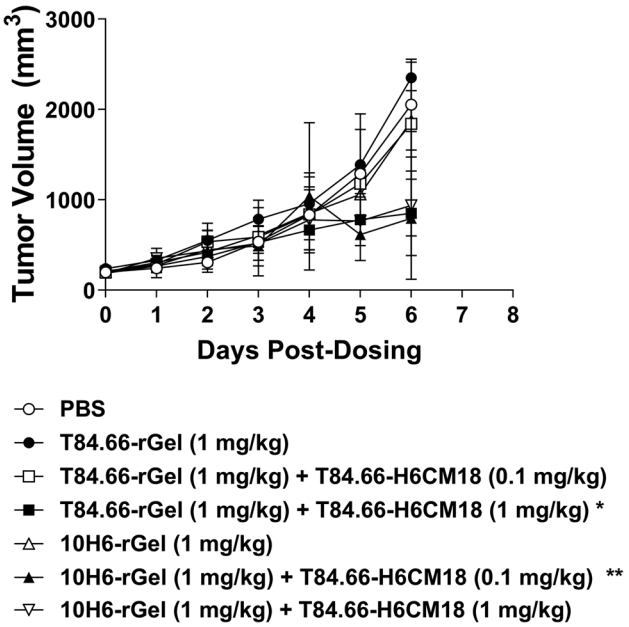

Fig. 5 T84.66-H6CM18 co-treatment improves response of LS174T xenografts to 10H6-rGel and T84.66-rGel. Mice were administered PBS (open circles), 1 mg/kg T84.66-rGel (black circles), 1 mg/kg T84.66-rGel + 0.1 mg/kg T84.66-H6CM18 (open squares), 1 mg/kg T84.66-rGel + 1 mg/kg T84.66-H6CM18 (closed squares), 1 mg/kg 10H6-rGel (open triangles), 1 mg/kg 10H6-rGel + 0.1 T84.66-H6CM18 (closed triangle), 1 mg/kg 10H6-rGel + 1 mg/kg T84.66-H6CM18 (inverse triangles). A Student's t-test was used to determine the statistical difference between treatment groups and PBS (*, $p = 0.0388$; **, $p = 0.0156$)

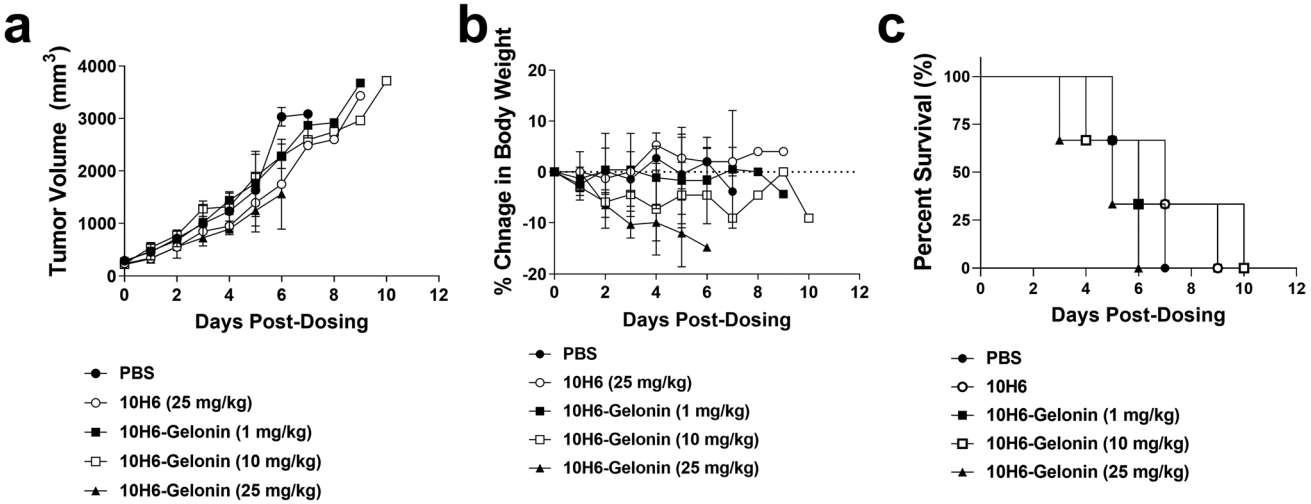

Fig. 4 10H6-rGel *in vivo* efficacy and toxicity in LS174T xenograft-bearing mice. **a** Tumor growth and **b** change in body weight of mice bearing LS174T-xenografts following response to PBS (closed circles), 25 mg/kg 10H6 (open circles), 1 mg/kg 10H6-rGel (closed squares), 10 mg/kg 10H6-rGel (open squares), and 25 mg/kg 10H6-rGel (closed triangle). Mice were administered treatments on Day 0. Symbols represent means while bars represent standard deviations of the mean. Dotted line represents 0% change in body weight. **c** Kaplan–Meier survival analysis in response to PBS (closed circles), 25 mg/kg 10H6 (open circles), 1 mg/kg 10H6-rGel (closed squares), 10 mg/kg 10H6-rGel (open squares), and 25 mg/kg 10H6-rGel (closed triangle)

growth as found in PBS treated mice. However, the combination of 1 mg/kg T84.66-H6CM18 with T84.66-gelonin (1 mg/kg) led to an approximate 50% decrease in tumor burden ($p = 0.0388$). The pH-dependent antibody immunotoxin, 10H6-rGel (1 mg/kg), in combination with 0.1 mg/kg T84.66-H6CM18, also demonstrated a ~ 50% decrease in average tumor burden when compared to results from mice receiving PBS or 10H6-rGel alone ($p = 0.0156$). Combinations of T84.66-rGel or 10H6-rGel with T84.66-H6CM18 did not cause any observable toxicity. Although the data presented in Fig. 5 describes tumor burden up to the day all PBS treated mice died, all other treatment groups were monitored continually until death, where tumor burden, weight loss, and survival are provided in Fig. S6. These data suggest a single bolus dose of the 10H6-rGel + T84.66-H6CM18 (0.1 or 1 mg/kg) was able to significantly delay growth of LS174T tumors in xenograft-bearing mice.

Multi-Dose Efficacy Evaluation

In order to pursue a more sustained response, we designed a multi-dose regimen for combination therapy with targeted gelonin and H6CM18, with intravenous injections administered every four days. PBS or 1 mg/kg of T84.66-H6CM18 were administered alone for comparison. With dosing every 4 days, animals treated with T84.66-H6CM18 alone demonstrated similar tumor growth as animals administered with PBS, suggesting no benefits from T84.66-H6CM18 administration (alone). Groups of mice treated with 10H6-rGel (1 mg/kg) in combination with T84.66-H6CM18 (0.1 mg/kg or 1 mg/kg) showed significant delays in tumor growth (Fig. 6a & Fig. S7). Consistent with findings from the single-dose co-administration, the multi-dose regimen did not lead to significant changes in mean body weight (Fig. 6b). The combination of 10H6-rGel and T84.66-H6CM18 (0.1 mg/kg) significantly extended the median survival of mice to 19.5 days, as compared to 13 days for PBS (**$p = 0.0072$) and 11 days for mice receiving T84.66-H6CM18 alone (***$p = 0.0005$) (Fig. 6c). 1 mg/kg of T84.66-H6CM18 in combination of 10H6-rGel significantly extended the median survival of mice to 22 days, as compared to the PBS (**$p = 0.0017$) and T84.66-H6CM18 alone (***$p = 0.0002$) (Fig. 6c). The combination of 10H6-rGel with 1 mg/kg T84.66-H6CM18 showed better overall performance than the combination of 10H6-rGel with 0.1 mg/kg T84.66-H6CM18, but the differences between the two treatment groups were not statistically significant.

DISCUSSION

In 1970, Moolten and Cooperband described the development of an antibody-diphtheria toxin conjugate that selectively lysed cells that were infected with the mumps virus (38). In the 40 years since the first reported IT, substantial efforts have been made to develop ITs for cancer therapy (1, 39, 40); however, clinical success has been limited. Poor IT efficacy against solid tumor cancers may relate to physical barriers that impede IT uptake and penetration (41–43), and to off-target toxicities that limit IT doses below those necessary to effectively treat tumors (3, 44). Gelonin, a type I RIP, is well-tolerated; however, gelonin based ITs generally demonstrate poor potency and clinical investigations failed to demonstrate anti-cancer efficacy (11). There have

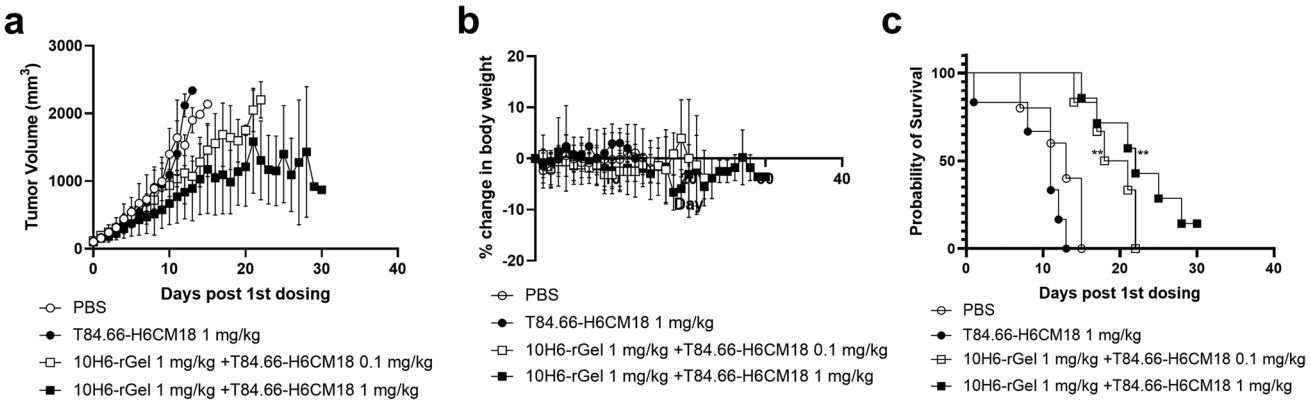

Fig. 6 Multidosing of T84.66-H6CM18 with 10H6-rGel increases the median survival of mice bearing LS174T xenografts. **a** Tumor growth and **b** change in body weight of mice bearing LS174T-xenografts following in response to PBS (open circles), 1 mg/kg T84.66-H6CM18 (closed circles), 1 mg/kg 10H6-rGel + 0.1 mg/kg T84.66-H6CM18 (open squares), 1 mg/kg 10H6-rGel + 1 mg/kg T84.66-H6CM18 (closed squares). Mice were administered treatments on Day 0, 4, 8, 12, 16, 20, 24, 28. Symbols represent means while bars represent standard deviations of the mean and asterisks note statistical significance from PBS. Dotted line represents 0% change in body weight. **c** Kaplan–Meier survival analysis in response to PBS (open circles), 1 mg/kg T84.66-H6CM18 (closed circles), 1 mg/kg 10H6-rGel + 0.1 mg/kg T84.66-H6CM18 (open squares), 1 mg/kg 10H6-rGel + 1 mg/kg T84.66-H6CM18 (closed squares)

been various strategies to improve the endosomal escape efficiency and potency of gelonin. Chemical endosomal escape enhancers including lysosomotropic amines, carboxylic ionophores, and calcium channel antagonists have enhanced the cytotoxicity of gelonin by 10 ~ 15 fold (45, 46), and wortmannin co-administration significantly potentiated bFGF-gelonin anti-tumor efficacy in mice (47). Shin et al. explored direct conjugation of a protein transduction domain, TAT, to gelonin and demonstrated enhanced *in vitro* potency by ~ 85-fold in various cancer cell models (48). Recently, photochemical internalization strategies have been developed to enhance gelonin potency *in vitro* and *in vivo*, including clinical investigations (49–54). To date, there are few reports of the development of targeted delivery systems, suitable for treatment of distant metastases, that enable substantially increased anti-cancer potency of gelonin. The Yang group pursued antibody-directed TAT-gelonin using an anti-CEA antibody, T84.66, and noncovalent, electrostatic TAT-heparin interaction to enable enhanced penetration of cancer cell plasma membranes following dissociation from heparin. Unfortunately, evaluation of this strategy using LS174T cells indicated no enhancement of gelonin potency (55). A second strategy, proposed by the Wittrup laboratory, used recombinant listeriolysin O (LLO) and gelonin fusion proteins, where fibronectins were employed to target either EGFR or CEA. When used in combination, the LLO fusion protein potentiated the potency of gelonin fusion proteins by more than 1,000-fold *in vitro* (56). However, toxicities and immunogenicity associated with LLO may complicate, or even preclude, development for *in vivo* application in humans.

The present strategy attempts to enhance therapeutic selectivity of IT by use of agents with the following properties: 1) little to no toxicity following treatment with the escape agent or toxin when administered alone; 2) vectors that allow delivery and release of the toxin and escape agent from the endosomal membranes of targeted cells; 3) escape agents capable of forming pores sufficient for passage of ≥ 30 kDa toxins; and 4) escape agents capable of rapid pore formation/membrane disruption in endosomes. With application of ideal targeting and escape agents, we have hypothesized that it will be possible to increase gelonin potency by more than 10,000-fold.

His-CM_{18}-PTD4 has been demonstrated to enable rapid translocation of macromolecules to the cytoplasm of cells in culture, presumably via the proton sponge effect (*vs.* via pore formation) (57–59). To enable enhanced delivery of macromolecular toxins to the cytoplasm of targeted cells, we employed a vc-PABC linker to conjugate H6CM18 to tumor-specific monoclonal antibodies. The vc-PABC linker is commonly used in antibody–drug conjugates, including the FDA-approved agent *brentuximab vedotin*. This linker undergoes cleavage by cathepsin B within late-endosomes and lysosomes, freeing the unstable PABC moiety, which undergoes 1,6-elimination with a loss of *p*-iminoquinone methide and CO_2 (i.e. self-immolation) in acidic conditions of endosomes and lysosomes (60, 61). This self-immolation of PABC then results in a "native" state H6CM18 peptide, which can freely interact with endosomal membranes and destabilizing endosomes. We hypothesized that this peptide may be ideal for our delivery strategies, as His-CM_{18}-PTD4 increased cytosolic delivery of CRISPR/Cas9 components and 250 kDa fluorescent dextrans following a 1–2-min incubation (57–59). Combinations with 10H6-nGel and T84.66-H6CM18 demonstrated a ~ 30-fold enhancement in potency. Fluorescent microscopy provided mechanistic evidence that the potency of 10H6-gelonin was potentiated by H6CM18 by increasing endosome escape. In order to observe an IC_{50} value 10^3–10^4 fold greater than gelonin, a high-affinity antibody (e.g., T84.66) may be required to promote antigen engagement and prevent rapid antigen dissociation. We tested this hypothesis using our strategy by combining T84.66-nGel with concentrations of T84.66-H6CM18 that achieve ~ 75% receptor occupancy (i.e., 25 pM). This co-treatment approach is similar to that employed by Pirie et al., which described use of competing targeting domains, with use of a targeted lytic agent at concentrations resulting in ~ 70% receptor occupancy (56). Their results demonstrated that targeted LLO fusion proteins enhanced the potency of anti-CEA gelonin immunotoxins from approximately 1 μM to 1 nM, and our combination strategy was found to yield similar results (i.e., 1,000- 6,000-fold enhancements in gelonin potency). However, unlike the LLO fusion proteins used by Pirie et al., our mAb-H6CM18 conjugates appear to be non-toxic.

It is important to note that we have not included in this work comparisons of the cytotoxicity of our combination approach when applied to cells expressing human CEA *vs.* when applied to cells that do not express CEA. However, our prior work has demonstrated on-target specificity of 10H6 and T84.66 through flow cytometry studies that showed substantial binding of each antibody to murine cancer cells expressing human CEA ($MC38^{CEA+}$), with no detectable binding to cells lacking CEA expression ($MC38^{CEA-}$) (22). Due to the low expression of human CEA in this transfected murine cell line, MC38 cells are not useful for evaluation of the efficacy of the co-delivery strategy described in this manuscript. We are not aware of a suitable cell pair for appropriate evaluation of a targeting index or for appropriate assessment of therapeutic selectivity in cell culture. However, demonstration of *in vivo* anti-tumor efficacy at dose-levels leading to no observable toxicity, as shown in the manuscript, likely provides the most meaningful evaluation of the therapeutic selectivity of our approach.

Prior work within our laboratory showed that the maximum tumor concentration of T84.66, following a 1 mg/kg

dose in LS174T xenograft-bearing mice, is ~ 10–30 nM (62). On average, gelonin immunoconjugates exhibit a twofold greater plasma clearance than the naked IgG molecule, without altering tumor selectivity (63). Considering this change in pharmacokinetics, it is possible the dose of 1 mg/kg gelonin ITs in LS174T would yield concentrations around the *in vitro* IC_{50} value (i.e. ~ 1 nM). Pharmacokinetic analyses of peptide conjugates in a mouse model of colorectal cancer (data not shown) determined conjugation of H6CM18 to 10H6 only led to minor alterations in the pharmacokinetics, with an increase in clearance by ~ 1.6-fold, but with no significant effect on tumor selectivity. Based on PK and cytotoxicity, we selected a 1 mg/kg mAb-gelonin dose + 0.1/1 mg/kg T84.66-H6CM18 for evaluation. Based on our tumor growth inhibition studies, immunotoxin treatment (alone) displayed no efficacy, along with T84.66-rGel + T84.66-H6CM18 at 0.1 mg/kg. The lack of efficacy for the latter treatment could be due to sub-optimal concentrations of T84.66-H6CM18 because of TMDD and competition with T84.66-rGel. However, increasing the dose of T84.66-H6CM18 to 1 mg/kg resulted in an efficacious response. Interestingly, the T84.66-H6CM18 + 10H6-rGel combinations demonstrated superior inhibition of tumor growth. Our original hypothesis suggested CAR mAbs can be utilized to achieve pH-dependent release of membrane-associated CEA, promoting diffusion or CAR-toxin past the membrane. Although our cross-linker is cleavable, the concentrations of glutathione within endosomes may be insufficient to reduce the disulfide bond. Therefore, pH-dependent release of CEA by 10H6 may allow improved delivery of gelonin into the cytosol, while T84.66-rGel remains bound to membrane-associated CEA (and, possibly, directed toward lysosomal catabolism). Additionally, the lower affinity of 10H6 compared to T84.66 could also increase tumor distribution, relative to T84.66-rGel, due to binding site barrier effects (64). However, further studies must be conducted to evaluate these hypotheses. Of note, our laboratory recently reported a strategy to overcome the binding site barrier using transient competitive inhibitors of mAb-antigen binding (65, 66). This approach may be evaluated in combination with ITs with high affinity antigen binding, such as T84.66-rGel, to evaluate the impact of heterogenous tumor penetration on IT efficacy.

As with all protein-based therapies, clinical application of our proposed combination therapy would bring some risk for toxicity and/or for reduced efficacy resulting from the development of host anti-drug antibodies (i.e., anti-antibody, anti-H6CM18, or anti-gelonin antibodies). Interestingly, no adverse effects relating to immunogenicity were reported following clinical evaluation of HUM-195/rGel, a gelonin immunotoxin, with administration of 10 mg/m^2 every 76–98 h for six courses of therapy (67). Although we did not attempt to assay for host anti-drug antibodies, development of such antibodies in our study is considered unlikely, owing to our use of NU/J homozygous immunodeficient mice, which lack T cells and show blunted B cell development. We plan to investigate host immune responses to our combination therapy in subsequent investigations through use of immunocompetent C57BL/6 mice (22).

The LS174T xenograft model employed in this study is well-known to be poorly responsive to monoclonal antibody-based therapy. For example, in our prior investigations, unconjugated 10H6 and unconjugated T84.66 demonstrated no effects on LS174T tumor growth (68). Shin et al. also found no significant effects on tumor growth following administration of T84.66 and T84.66-Gel conjugates to mice with LS174T xenografts (69). Similar results (lack of substantial efficacy) in this model have been shown following treatment with labetuzumab (70) and cetuximab (71–73). When evaluated in context with prior investigations of monoclonal antibodies in the LS174T mouse model, the 50% tumor burden reduction and 69% survival extension observed for our combination therapy may be considered to be quite promising.

CONCLUSION

In summary, our work demonstrated 10^3–10^4-fold enhancement of gelonin potency with conjugation to a specific anti-tumor antigen antibody and with cotreatment with targeted delivery of an endosomal escape peptide (H6CM18). Importantly, we employed a protease cleavable and self-immolative linker (i.e. vc-PABC) that enables release of native peptide within late endosomes. CAR mAbs showed promise *in vivo* when combined with high affinity, T84.66-H6CM18 peptide conjugates, reducing tumor burden by ~ 50% and increasing survival duration by ~ 70%. These studies provide positive initial evidence, demonstrating significant anti-tumor effects and low toxicity, which supports further development of strategies for co-administration of antibody conjugates enabling targeted delivery RIPs and endosomal escape peptides.

Supplementary Information The online version contains supplementary material available at https://doi.org/10.1208/s12248-022-00698-x.

Acknowledgements The authors would like to thank Jacobs School of Medicine and Biomedical Sciences for the use of Leica DMi 8 inverted fluorescence microscope for live cell imaging.

Author Contribution J.R.P. and J.P.B. contributed to conceptualization; J.R.P. and P.C. contributed to methodology; J.R.P and P.C. contributed to investigation; J.R.P. contributed to writing—original draft preparation; J.R.P., P.C., B.M.B. and J.P.B. contributed to writing—review and editing; J.P.B. contributed to funding acquisition; J.P.B. provided the resources; J.P.B. contributed to supervision.

Funding This work was supported by the National Cancer Institute of National Institutes of Health (grant numbers CA204192 and CA246785).

Declarations

Conflict of Interest Disclosure Statement J.P.B. serves as the Director of the University at Buffalo Center for Protein Therapeutics, which is supported by an industry consortium. Through the consortium, J.P.B. has received research support, for work unrelated to this report, from Abbvie, Amgen, CSL-Behring, Eli Lilly, Genentech, GSK, Janssen, Merck, Roche, and Sanofi. During the course of this work, J.P.B. has received consulting fees from companies involved with the development of cancer therapies, including: Abbvie, Amgen, Eli Lilly, Merck, and Pfizer

Ethical Approval Protocols for animal experiments were approved by the Institutional Animal Use and Care Committee of the University at Buffalo (PHC44086Y).

References

1. FitzGerald DJ, Kreitman R, Wilson W, Squires D, Pastan I. Recombinant immunotoxins for treating cancer. Int J Med Microbiol. 2004;293(7–8):577–82.
2. Kreitman RJ. Recombinant immunotoxins for the treatment of chemoresistant hematologic malignancies. Curr Pharm Des. 2009;15(23):2652–64.
3. Alewine C, Hassan R, Pastan I. Advances in anticancer immunotoxin therapy. Oncologist. 2015;20(2):176–85.
4. Frankel AE, Houston LL, Issell BF, Fathman G. Prospects for immunotoxin therapy in cancer. Annu Rev Med. 1986;37:125–42.
5. Walsh MJ, Dodd JE, Hautbergue GM. Ribosome-inactivating proteins: potent poisons and molecular tools. Virulence. 2013;4(8):774–84.
6. de Virgilio M, Lombardi A, Caliandro R, Fabbrini MS. Ribosome-inactivating proteins: from plant defense to tumor attack. Toxins (Basel). 2010;2(11):2699–737.
7. Eiklid K, Olsnes S, Pihl A. Entry of lethal doses of abrin, ricin and modeccin into the cytosol of HeLa cells. Exp Cell Res. 1980;126(2):321–6.
8. Lambert JM, Blattler WA, McIntyre GD, Goldmacher VS, Scott CF. Immunotoxins containing single chain ribosome-inactivating proteins. In: Frankel AE, editor. Immunotoxins: Kluwer Academic Publishers; 1988. p. 180.
9. Taylor NS, Pollack M. Purification of Pseudomonas aeruginosa exotoxin by affinity chromatography. Infect Immun. 1978;19(1):66–70.
10. Lyu MA, Cao YJ, Mohamedali KA, Rosenblum MG. Cell-targeting fusion constructs containing recombinant gelonin. Methods Enzymol. 2012;502:167–214.
11. Borthakur G, Rosenblum MG, Talpaz M, Daver N, Ravandi F, Faderl S, *et al*. Phase 1 study of an anti-CD33 immunotoxin, humanized monoclonal antibody M195 conjugated to recombinant gelonin (HUM-195/rGEL), in patients with advanced myeloid malignancies. Haematologica. 2013;98(2):217–21.
12. Pirie CM, Hackel BJ, Rosenblum MG, Wittrup KD. Convergent potency of internalized gelonin immunotoxins across varied cell lines, antigens, and targeting moieties. J Biol Chem. 2011;286(6):4165–72.
13. Yazdi PT, Murphy RM. Quantitative analysis of protein synthesis inhibition by transferrin-toxin conjugates. Cancer Res. 1994;54(24):6387–94.
14. Copolovici DM, Langel K, Eriste E, Langel U. Cell-penetrating peptides: design, synthesis, and applications. ACS Nano. 2014;8(3):1972–94.
15. Guidotti G, Brambilla L, Rossi D. Cell-Penetrating Peptides: From Basic Research to Clinics. Trends Pharmacol Sci. 2017;38(4):406–24.
16. Haas DH, Murphy RM. Design of a pH-sensitive pore-forming peptide with improved performance. J Pept Res. 2004;63(1):9–16.
17. Li W, Nicol F, Szoka FC Jr. GALA: a designed synthetic pH-responsive amphipathic peptide with applications in drug and gene delivery. Adv Drug Deliv Rev. 2004;56(7):967–85.
18. Parente RA, Nir S, Szoka FC Jr. Mechanism of leakage of phospholipid vesicle contents induced by the peptide GALA. Biochemistry. 1990;29(37):8720–8.
19. Junghans R, Waldmann T. Metabolism of Tac (IL2Ralpha): physiology of cell surface shedding and renal catabolism, and suppression of catabolism by antibody binding. J Exp Med. 1996;183(4):1587–602.
20. Igawa T, Ishii S, Tachibana T, Maeda A, Higuchi Y, Shimaoka S, *et al*. Antibody recycling by engineered pH-dependent antigen binding improves the duration of antigen neutralization. Nat Biotechnol. 2010;28(11):1203–7.
21. Chaparro-Riggers J, Liang H, Devay RM, Bai L, Sutton JE, Chen W, *et al*. Increasing Serum Half-life and Extending Cholesterol Lowering *in vivo* by Engineering Antibody with pH-sensitive Binding to PCSK9. J Biol Chem. 2012;287(14):11090–7.
22. Engler FA, Polli JR, Li T, An B, Otteneder M, Qu J, *et al*. "Catch-and-Release" Anti-Carcinoembryonic Antigen Monoclonal Antibody Leads to Greater Plasma and Tumor Exposure in a Mouse Model of Colorectal Cancer. J Pharmacol Exp Ther. 2018;366(1):205–19.
23. Shi ZR, Tsao D, Kim YS. Subcellular distribution, synthesis, and release of carcinoembryonic antigen in cultured human colon adenocarcinoma cell lines. Cancer Res. 1983;43(9):4045–9.
24. Levin LV, Griffin TW, Childs LR, Davis S, Haagensen DE Jr. Comparison of multiple anti-CEA immunotoxins active against human adenocarcinoma cells. Cancer Immunol Immunother. 1987;24(3):202–6.
25. Hermanson GT. Bioconjugate techniques. Third edition. ed. London ; Waltham, MA: Elsevier/AP; 2013. xvii, 1146 pages p.
26. Engler FA, Balthasar JP. Development and validation of an enzyme-linked immunosorbent assay for the quantification of gelonin in mouse plasma. J Immunoassay Immunochem. 2016;37(6):611–22.
27. Eeftens JM, van der Torre J, Burnham DR, Dekker C. Copper-free click chemistry for attachment of biomolecules in magnetic tweezers. BMC Biophys. 2015;8:9.
28. Dunn KW, Kamocka MM, McDonald JH. A practical guide to evaluating colocalization in biological microscopy. Am J Physiol Cell Physiol. 2011;300(4):C723–42.
29. Bolte S, Cordelières FP. A guided tour into subcellular colocalization analysis in light microscopy. J Microsc. 2006;224(Pt 3):213–32.
30. Salomone F, Breton M, Leray I, Cardarelli F, Boccardi C, Bonhenry D, *et al*. High-yield nontoxic gene transfer through conjugation of the CM_{18}-Tat_{11} chimeric peptide with nanosecond electric pulses. Mol Pharm. 2014;11(7):2466–74.
31. Salomone F, Cardarelli F, Di Luca M, Boccardi C, Nifosì R, Bardi G, *et al*. A novel chimeric cell-penetrating peptide with membrane-disruptive properties for efficient endosomal escape. J Control Release. 2012;163(3):293–303.
32. Del'Guidice T, Lepetit-Stoffaes JP, Bordeleau LJ, Roberge J, Théberge V, Lauvaux C, *et al*. Membrane permeabilizing

amphiphilic peptide delivers recombinant transcription factor and CRISPR-Cas9/Cpf1 ribonucleoproteins in hard-to-modify cells. PLoS One. 2018;13(4):e0195558.
33. King HD, Dubowchik GM, Mastalerz H, Willner D, Hofstead SJ, Firestone RA, *et al*. Monoclonal antibody conjugates of doxorubicin prepared with branched peptide linkers: inhibition of aggregation by methoxytriethyleneglycol chains. J Med Chem. 2002;45(19):4336–43.
34. Oyama K, Takabayashi M, Takei Y, Arai S, Takeoka S, Ishiwata S, *et al*. Walking nanothermometers: spatiotemporal temperature measurement of transported acidic organelles in single living cells. Lab Chip. 2012;12(9):1591–3.
35. Shi B, Huang Q-Q, Birkett R, Doyle R, Dorfleutner A, Stehlik C, *et al*. SNAPIN is critical for lysosomal acidification and autophagosome maturation in macrophages. Autophagy. 2017;13(2):285–301.
36. Scott CF Jr, Goldmacher VS, Lambert JM, Chari RV, Bolender S, Gauthier MN, *et al*. The antileukemic efficacy of an immunotoxin composed of a monoclonal anti-Thy-1 antibody disulfide linked to the ribosome-inactivating protein gelonin. Cancer Immunol Immunother. 1987;25(1):31–40.
37. Scott CF Jr, Lambert JM, Goldmacher VS, Blatter WA, Sobel R, Schlossman SF, *et al*. The pharmacokinetics and toxicity of murine monoclonal antibodies and of gelonin conjugates of these antibodies. Int J Immunopharmacol. 1987;9(2):211–25.
38. Moolten FL, Cooperband SR. Selective destruction of target cells by diphtheria toxin conjugated to antibody directed against antigens on the cells. Science. 1970;169(3940):68–70.
39. Pastan I, Hassan R, FitzGerald DJ, Kreitman RJ. Immunotoxin therapy of cancer. Nat Rev Cancer. 2006;6(7):559–65.
40. Akbari B, Farajnia S, AhdiKhosroshahi S, Safari F, Yousefi M, Dariushnejad H, *et al*. Immunotoxins in cancer therapy: Review and update. Int Rev Immunol. 2017;36(4):207–19.
41. Bordeau BM, Balthasar JP. Strategies to enhance monoclonal antibody uptake and distribution in solid tumors. Cancer Biol Med. 2021;18(3):649–64.
42. Shan L, Liu Y, Wang P. Recombinant Immunotoxin Therapy of Solid Tumors: Challenges and Strategies. J Basic Clin Med. 2013;2(2):1–6.
43. Pastan I, Hassan R, FitzGerald DJ, Kreitman RJ. Immunotoxin Treatment of Cancer. Annu Rev Med. 2007;58(1):221–37.
44. Posey JA, Khazaeli MB, Bookman MA, Nowrouzi A, Grizzle WE, Thornton J, *et al*. A Phase I Trial of the Single-Chain Immunotoxin SGN-10 (BR96 sFv-PE40) in Patients with Advanced Solid Tumors. Clin Cancer Res. 2002;8(10):3092–9.
45. Marcil J, Ravindranath N, Sairam MR. Cytotoxic activity of lutropin-gelonin conjugate in mouse Leydig tumor cells: Potentiation of the hormonotoxin activity by different drugs. Mol Cell Endocrinol. 1993;92(1):83–90.
46. Mujoo K, Reisfeld RA, Cheung L, Rosenblum MG. A potent and specific immunotoxin for tumor cells expressing disialoganglioside GD2. Cancer Immunol Immunother. 1991;34(3):198–204.
47. Davol PA, Bizuneh A, Frackelton AR. Wortmannin, a phosphoinositide 3-kinase inhibitor, selectively enhances cytotoxicity of receptor-directed-toxin chimeras *in vitro* and *in vivo*. Anticancer Res. 1999;19(3A):1705–13.
48. Shin MC, Zhao J, Zhang J, Huang Y, He H, Wang M, *et al*. Recombinant TAT-gelonin fusion toxin: synthesis and characterization of heparin/protamine-regulated cell transduction. J Biomed Mater Res A. 2015;103(1):409–19.
49. Berstad MB, Cheung LH, Berg K, Peng Q, Fremstedal ASV, Patzke S, *et al*. Design of an EGFR-targeting toxin for photochemical delivery: *in vitro* and *in vivo* selectivity and efficacy. Oncogene. 2015;34(44):5582–92.
50. Berg K, Høgset A, Prasmickaite L, Weyergang A, Bonsted A, Dietze A, *et al*. Photochemical internalization (PCI): A novel technology for activation of endocytosed therapeutic agents. Med Laser Appl. 2006;21(4):239–50.
51. Dietze A, Peng Q, Selbo PK, Kaalhus O, Müller C, Bown S, *et al*. Enhanced photodynamic destruction of a transplantable fibrosarcoma using photochemical internalisation of gelonin. Br J Cancer. 2005;92(11):2004–9.
52. Selbo PK, Sivam G, Fodstad Ø, Sandvig K, Berg K. *In vivo* documentation of photochemical internalization, a novel approach to site specific cancer therapy. Int J Cancer. 2001;92(5):761–6.
53. Bull-Hansen B, Berstad MB, Berg K, Cao Y, Skarpen E, Fremstedal AS, *et al*. Photochemical activation of MH3-B1/rGel: a HER2-targeted treatment approach for ovarian cancer. Oncotarget. 2015;6(14):12436–51.
54. Weyergang A, Fremstedal AS, Skarpen E, Peng Q, Mohamedali KA, Eng MS, *et al*. Light-enhanced VEGF121/rGel: A tumor targeted modality with vascular and immune-mediated efficacy. J Control Release. 2018;288:161–72.
55. Shin MC, Zhang J, Min KA, He H, David AE, Huang Y, *et al*. PTD-Modified ATTEMPTS for Enhanced Toxin-based Cancer Therapy: An *In vivo* Proof-of-Concept Study. Pharm Res. 2015;32(8):2690–703.
56. Pirie CM, Liu DV, Wittrup KD. Targeted cytolysins synergistically potentiate cytoplasmic delivery of gelonin immunotoxin. Mol Cancer Ther. 2013;12(9):1774–82.
57. Salomone F, Breton M, Leray I, Cardarelli F, Boccardi C, Bonhenry D, *et al*. High-yield nontoxic gene transfer through conjugation of the CM(1)(8)-Tat(1)(1) chimeric peptide with nanosecond electric pulses. Mol Pharm. 2014;11(7):2466–74.
58. Salomone F, Cardarelli F, Di Luca M, Boccardi C, Nifosi R, Bardi G, *et al*. A novel chimeric cell-penetrating peptide with membrane-disruptive properties for efficient endosomal escape. J Control Release. 2012;163(3):293–303.
59. Del Guidice T, Lepetit-Stoffaes JP, Bordeleau LJ, Roberge J, Theberge V, Lauvaux C, *et al*. Membrane permeabilizing amphiphilic peptide delivers recombinant transcription factor and CRISPR-Cas9/Cpf1 ribonucleoproteins in hard-to-modify cells. Plos One. 2018;13(4).
60. Dubowchik GM, Firestone RA, Padilla L, Willner D, Hofstead SJ, Mosure K, *et al*. Cathepsin B-labile dipeptide linkers for lysosomal release of doxorubicin from internalizing immunoconjugates: model studies of enzymatic drug release and antigen-specific *in vitro* anticancer activity. Bioconjug Chem. 2002;13(4):855–69.
61. Dubowchik GM, Mosure K, Knipe JO, Firestone RA. Cathepsin B-sensitive dipeptide prodrugs. 2. Models of anticancer drugs paclitaxel (Taxol), mitomycin C and doxorubicin. Bioorg Med Chem Lett. 1998;8(23):3347–52.
62. Abuqayyas L, Balthasar JP. Application of PBPK modeling to predict monoclonal antibody disposition in plasma and tissues in mouse models of human colorectal cancer. J Pharmacokinet Pharmacodyn. 2012;39(6):683–710.
63. Mujoo K, Cheung L, Murray JL, Rosenblum MG. Pharmacokinetics, tissue distribution, and *in vivo* antitumor effects of the antimelanoma immunotoxin ZME-gelonin. Cancer Immunol Immunother. 1995;40(5):339–45.
64. Fujimori K, Covell DG, Fletcher JE, Weinstein JN. A modeling analysis of monoclonal antibody percolation through tumors: a binding-site barrier. J Nucl Med. 1990;31(7):1191–8.
65. Bordeau BM, Yang Y, Balthasar JP. Transient Competitive Inhibition Bypasses the Binding Site Barrier to Improve Tumor Penetration of Trastuzumab and Enhance T-DM1 Efficacy. Cancer Res. 2021;81(15):4145–54.

66. Bordeau BM, Abuqayyas L, Nguyen TD, Chen P, Balthasar JP. Development and Evaluation of Competitive Inhibitors of Trastuzumab-HER2 Binding to Bypass the Binding-Site Barrier. Front Pharmacol. 2022;13.
67. Caron PC, Jurcic JG, Scott AM, Finn RD, Divgi CR, Graham MC, *et al*. A phase 1B trial of humanized monoclonal antibody M195 (anti-CD33) in myeloid leukemia: specific targeting without immunogenicity. Blood. 1994;83(7):1760–8.
68. Urva SR, Yang VC, Balthasar JP. Physiologically based pharmacokinetic model for T84.66: a monoclonal anti-CEA antibody. J Pharm Sci. 2010;99(3):1582–600.
69. Shin MC, Zhang J, Ah Min K, Lee K, Moon C, Balthasar JP, *et al*. Combination of antibody targeting and PTD-mediated intracellular toxin delivery for colorectal cancer therapy. J Control Release. 2014;194:197–210.
70. Blumenthal RD, Osorio L, Hayes MK, Horak ID, Hansen HJ, Goldenberg DM. Carcinoembryonic antigen antibody inhibits lung metastasis and augments chemotherapy in a human colonic carcinoma xenograft. Cancer Immunol Immunother. 2005;54(4):315–27.
71. Vassileva V, Rajkumar V, Mazzantini M, Robson M, Badar A, Sharma S, *et al*. Significant Therapeutic Efficacy with Combined Radioimmunotherapy and Cetuximab in Preclinical Models of Colorectal Cancer. J Nucl Med. 2015;56(8):1239–45.
72. Kato J, Futamura M, Kanematsu M, Gaowa S, Mori R, Tanahashi T, et al. Combination therapy with zoledronic acid and cetuximab effectively suppresses growth of colorectal cancer cells regardless of KRAS status. Int J Cancer. 2016;138(6):1516–27.
73. Saridaki Z, Georgoulias V, Souglakos J. Mechanisms of resistance to anti-EGFR monoclonal antibody treatment in metastatic colorectal cancer. World J Gastroenterol. 2010;16(10):1177–87.